Journal of Earth Science, Vol. 21, No. 5, p. 782–791, October 2010
Printed in China
DOI: 10.1007/s12583-010-0112-2

ISSN 1674-487X

Pressure and Temperature Dependences of Elastic Properties of Grossular Garnet up to 17 GPa and 1 650 K

Yoshio Kono*, Steeve Gréaux
Geodynamics Research Center, Ehime University, Matsuyama 790-8577, *Japan*
Yuji Higo
JASRI, 1-1-1 *Mikazuki-cho, Sayo-gun, Hyogo* 679-5198, *Japan*
Hiroaki Ohfuji, Tetsuo Irifune
Geodynamics Research Center, Ehime University, Matsuyama 790-8577, *Japan*

ABSTRACT: Simultaneous ultrasonic elastic wave velocity and in situ synchrotron X-ray measurements on grossular garnet were carried out up to 17 GPa and 1 650 K. P- and S-wave velocities and bulk and shear modulus showed linear pressure and temperature dependence. These data yielded a pressure derivative of the bulk modulus of 4.42(7) and a shear modulus of 1.27(3), which are in good agreement with those of garnets with variable chemical compositions. Temperature dependence of the bulk modulus of grossular (-1.36×10^{-2} GPa/K) is also similar to that of other garnets, while the temperature dependence of the shear modulus of grossular (-1.11×10^{-2} GPa/K) is higher than those of magnesium end-member garnets and pyrolitic garnet.

KEY WORDS: elastic property, grossular, garnet, high pressure, high temperature.

INTRODUCTION

Garnet is one of the most abundant mineral constituents in the earth's upper mantle to mantle transition region, and, therefore, understanding the elastic wave velocities of garnets and their solid solutions would provide strong constraints on the structure and composition of this region from seismological views. Elastic properties of several garnet end-members and solid solutions have been extensively investigated by a number of studies at room pressure and temperature conditions (e.g., Sinogeikin and Bass, 2000; O'Neill et al., 1991, 1989; Bass, 1989). In contrast, the pressure and temperature dependences of the elastic properties of garnets is still not well understood. Elastic properties of Mg, Al end-member garnet (pyrope) have been relatively well investigated at high pressures and/or high temperatures in both direct elasticity measurements such as ultrasonic (e.g., Gwanmesia et al., 2006) or Brillouin scattering measurements (e.g., Sinogeikin and Bass, 2002, 2000) and pressure-volume-temperature (*PVT*) measurements (e.g., Wang et al., 1998). The pressure and temperature dependences of the elastic properties of pyrope determined by these methods are consistent with each other.

In contrast, the pressure and temperature dependences of other garnets with variable chemical

---

This study was supported by the research proposal to SPring-8 by Y Kono (No. 2007B1648), the Grant-in-Aid for Scientific Research from the Japanese Government to T Irifune.

*Corresponding author: kono@sci.ehime-u.ac.jp

Manuscript received February 22, 2010.
Manuscript accepted April 10, 2010.

compositions has not been well understood. Since calcium is one of the most abundant elements in the upper mantle, some studies have investigated the pressure and temperature dependences of the elastic properties of grossular garnets (e.g., Pavese et al., 2001; Conrad et al., 1999; Zhang et al., 1999; Isaak et al., 1992). However, the pressure and temperature dependences of the elastic properties of grossular remains controversial. In particular, the pressure dependence of the bulk modulus has been investigated in a number of studies (Pavese et al., 2001; Conrad et al., 1999; Zhang et al., 1999), but the results conflict with each other. Conrad et al. (1999) and Zhang et al. (1999) suggested that the pressure dependence of the bulk modulus is higher than 5 from Brillouin scattering and *PVT* measurements, respectively, in the diamond anvil cell. In addition, Olijnyk et al. (1991) showed the pressure dependence of the bulk modulus to be higher than 6. In contrast, Pavese et al. (2001) showed a low value for the pressure dependence of the bulk modulus (less than 4) from *PVT* measurements in the Paris-Edinburgh cell. Furthermore, an Ab initio calculation study showed pressure dependence of bulk modulus of 4.3 (Nobes et al., 2000).

Since *PVT* measurement is an indirect method to determine the pressure dependence of the bulk modulus, direct measurement should clarify this issue. Although Conrad et al. (1999) have directly measured the pressure dependence of the bulk modulus by Brillouin scattering measurements, they carried out only 5 measurements at pressures up to 10 GPa. Here we carried out further direct measurements, which are essential to clarify the pressure dependence of the bulk modulus of grossular. We investigated both pressure and temperature dependences of grossular garnet ($Ca_3Al_2Si_3O_{12}$) up to ~17 GPa and 1 650 K.

EXPERIMENTAL PROCEDURES AND SAMPLE DESCRIPTIONS

The P- (V_P) and S-wave (V_S) velocity measurements were performed for a hot-pressed polycrystalline grossular. The hot isostatic pressing was carried out at ~7 GPa and ~1 673 K for 2 h using a 3 000-ton high-pressure apparatus (Orange-3000) at GRC, Ehime University (cf., Higo et al., 2006). The starting material used was a glass with a grossular composition (CaO=37.14 wt.%, Al_2O_3=21.12 wt.%, SiO_2=40.70 wt.%), which was measured by energy-dispersive X-ray spectrometry with scanning electron microscopy. The hot-pressed sample was cut to ~1.5 mm length, and both ends of the sample were polished to 1 μm using diamond paste.

Simultaneous ultrasonic V_P and V_S measurements and X-ray radiography and diffraction experiments on polycrystalline grossular were carried out at the BL04B1 beamline at SPring-8, Japan. The unit-cell volume of the sample and pressure standard material was determined by energy-dispersive X-ray diffraction measurements with a Ge solid-state detector. The Ge solid-state detector was calibrated using the characteristic X-rays from metal standards (Cu, Ag, Mo, Ta, Pt, Au, and Pb). The diffraction angle was fixed at 5° using a calibration with diffraction lines of Au before the experiments. We determined the pressure from the equation of state of gold (Tsuchiya, 2003).

High-pressure and high-temperature experiments were performed using a 1 500-ton multi-anvil apparatus with a Kawai-type high-pressure vessel in the BL04B1 beamline. We used tungsten carbide anvils with a truncated edge length of 7 mm and MgO+17% CoO octahedron pressure medium with an edge length of 14 mm (Fig. 1a). We used MgO and NaCl sleeves as the sample container to realize a quasi-hydrostatic environment. In order to further reduce the deviatoric stress, we carried out the measurements after heating. A platinum foil tube heater was used. Temperature was monitored with a W3%Re–W25%Re thermocouple placed on the opposite side of the sample for measuring the temperature comparable to the center position of the sample.

Ultrasonic V_P and V_S measurements were conducted using the pulse reflection method. Both P- and S-wave signals were generated and received by a 10°Y-cut $LiNbO_3$ transducer (e.g., Li et al., 2004; Sinelnikov et al., 2004). A disk-shaped $LiNbO_3$ transducer (0.05-mm thickness and 3.2-mm diameter) with a resonant frequency of 60 MHz for P-waves and 40 MHz for S-waves was mounted on the backside of a WC anvil (cf., Higo et al., 2009). A series of reflected P- and S-wave signals from the interfaces of anvil/buffer rod (R0), buffer rod/sample (R1), and sample/backing material (mixture of NaCl, Au, and BN) (R2)

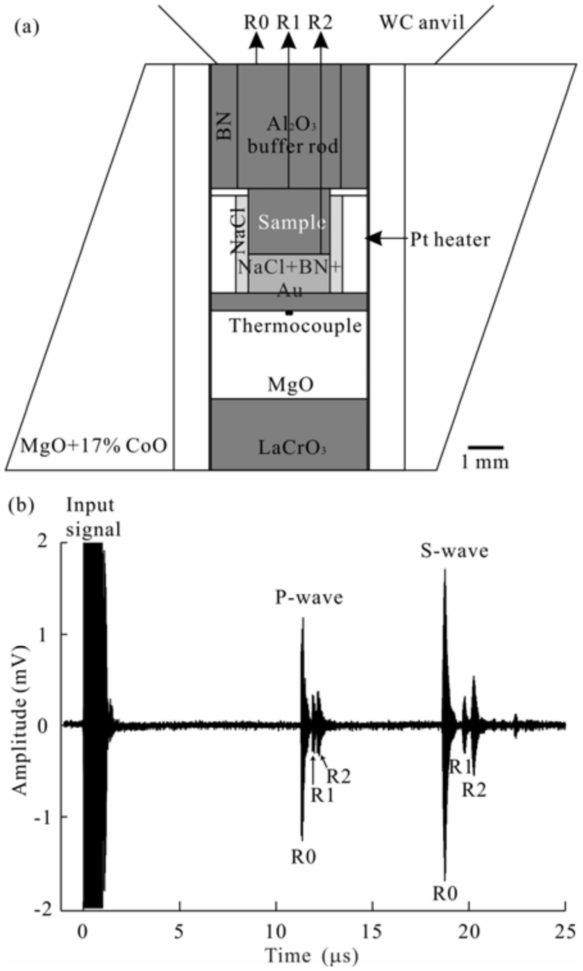

Figure 1. An illustration of the cell assembly used in the present experiments (a), and an example of P- and S-wave forms obtained at 16.9 GPa and 1 650 K with a 40-MHz input signal. R0, R1, and R2 represent P- and/or S-wave signals reflected from the interface of anvil/buffer rod, buffer rod/sample, and sample/backing material, respectively.

were acquired with a sampling rate of 5×10^9 points/second (0.2 ns at each data point) (Fig. 1b). The P- and S-wave travel times were determined by the pulse echo overlap method using the reflected signals from the buffer rod/sample (R1) and sample/backing material interfaces (R2).

The sample lengths at high pressures and high temperatures were directly determined from the X-ray radiography image using a high-resolution CCD camera. The high-resolution CCD camera has a resolution of 1 pixel=~2 μm. Both ends of the sample were marked by gold foils (2.5 μm thickness), which have a strong X-ray absorption (e.g., Higo et al., 2009; Li et al., 2004). Sample length was determined by analyzing the positions of the gold foils from the image (cf., Higo et al., 2009).

Then V_P and V_S were determined from the observed P- and/or S-wave travel times and sample length at each pressure and temperature condition. The uncertainty in determining P- and S-wave travel times of 0.2 ns causes up to 0.17% and 0.10% uncertainties in V_P and V_S, respectively. In contrast, uncertainty in the determination of sample length (2 μm) yields uncertainties of 0.16% in both V_P and V_S. The overall uncertainty in the present V_P and V_S determination is up to ±0.33% for V_P and ±0.26% for V_S. The resultant uncertainties in bulk and shear moduli are ±1.2% and ±0.5%, respectively.

The V_P and V_S measurements were carried out up to ~17 GPa and 1 650 K. We carried out two experiments. V_P and V_S data at 300 K were collected under the pressure conditions of ~5–9 GPa after heating to ~1 273 K. High-temperature V_P and V_S data were obtained at pressures between ~8 and 17 GPa up to 1 650 K for three heating cycles. Figure 2a shows X-ray diffraction patterns of the sample and pressure standard materials (NaCl and Au), which were placed at the back-ends of the sample. The X-ray diffraction pattern obtained at the highest pressure and temperature conditions shows that the sample consists only of polycrystalline grossular garnet, and no other phase was found in the X-ray diffraction pattern. We further investigated the recovered sample using a field-emission scanning electron microprobe (Fig. 2b). The data show that garnet with a grossular composition has a small grain size of ~1–2 μm even after high-pressure and high-temperature V_P and V_S measurements. We found an aluminum-depleted calcium silicate in the recovered sample. However, the amount of the phase is very minor, and we consider that the phase does not influence the pressure and temperature dependences of V_P, V_S, and elastic properties.

RESULTS AND DISCUSSION

Figure 3 shows P-wave (V_P) and S-wave (V_S) velocities, and adiabatic bulk (K_S) and shear (G) modulus of polycrystalline grossular at pressures up to 16.9 GPa and temperatures between 300 and 1 650 K (original data: Table 1). The data show a linear pres-

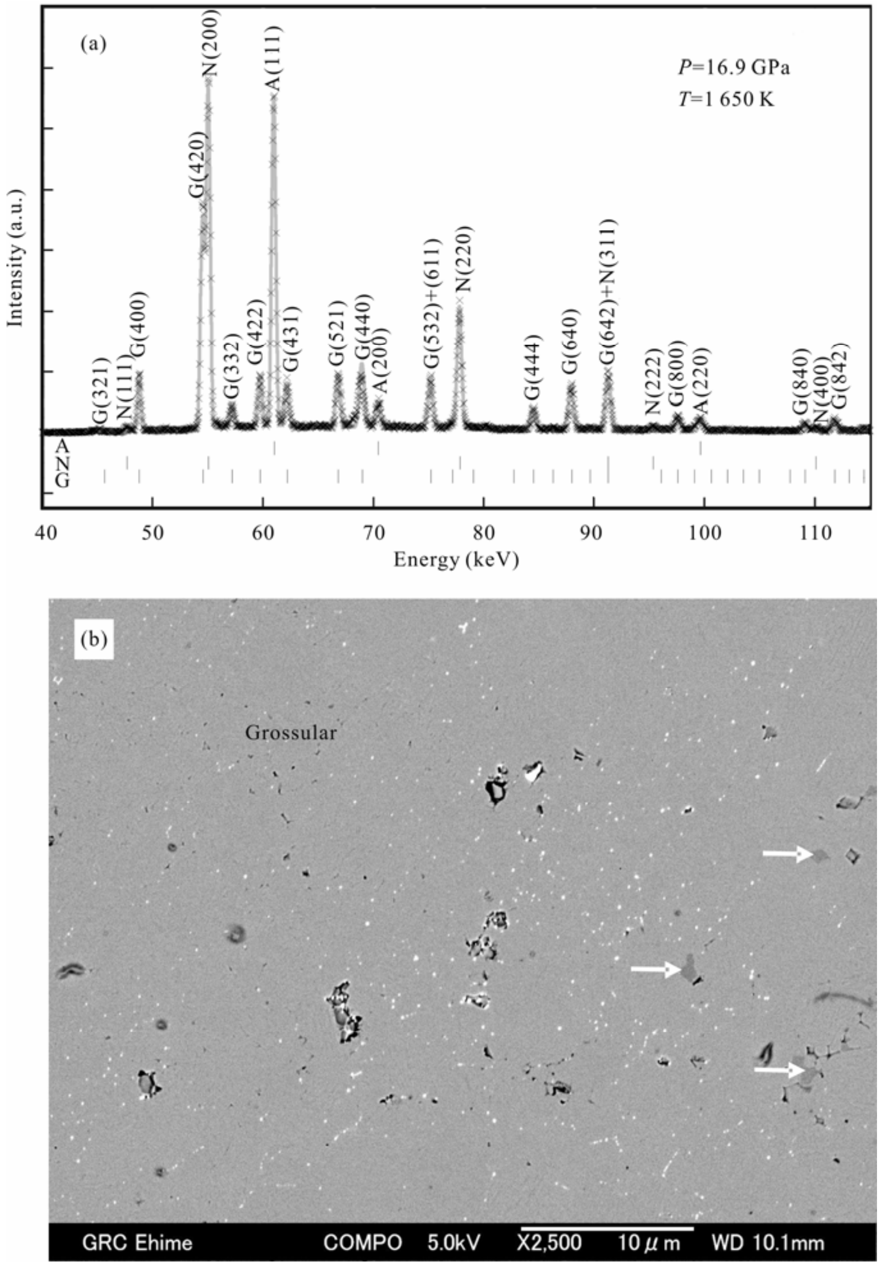

Figure 2. (a) Energy-dispersive X-ray diffraction pattern of grossular (G) and pressure standards (A. gold, N. NaCl) collected at 16.9 GPa and 1 650 K; (b) back-scattered electron image of the sample recovered from a V_P and V_S measurement. Arrows indicate minor amounts of aluminum-depleted calcium silicate phase (dark color).

sure and temperature dependences in both V_P and V_S, in contrast to the significantly non-linear temperature dependences of V_P and V_S observed for pyrolitic garnet (Irifune et al., 2008) using the same technique. A two-dimensional (P and T) linear fitting for V_P and V_S yields the equations V_P=9.389(1)+5.79(10)×10^{-2}×P–2.79(7)×10^{-4}×(T–300) and V_S=5.482(7)+1.68(6)×10^{-2}×P–2.09(4)×10^{-4}×(T–300), where P is the pressure in GPa; and T is the temperature in Kelvin (K). Numbers in parentheses represent errors in the linear fitting. K_S and G also show linear pressure and temperature dependences. A two-dimensional (P and T) linear fitting for K_S and G shows the equations K_S=171.5(8)+4.42(7)×P–1.36(4)×10^{-2}×(T–300) and G=108.4(3)+1.27(3)×P–1.11(2)×10^{-2}×(T–300). The experimental results are well reproduced by these equations, and the root mean square (RMS) misfit values are 0.17% for V_P, 0.18% for V_S, 0.55% for K_S, and 0.44% for G.

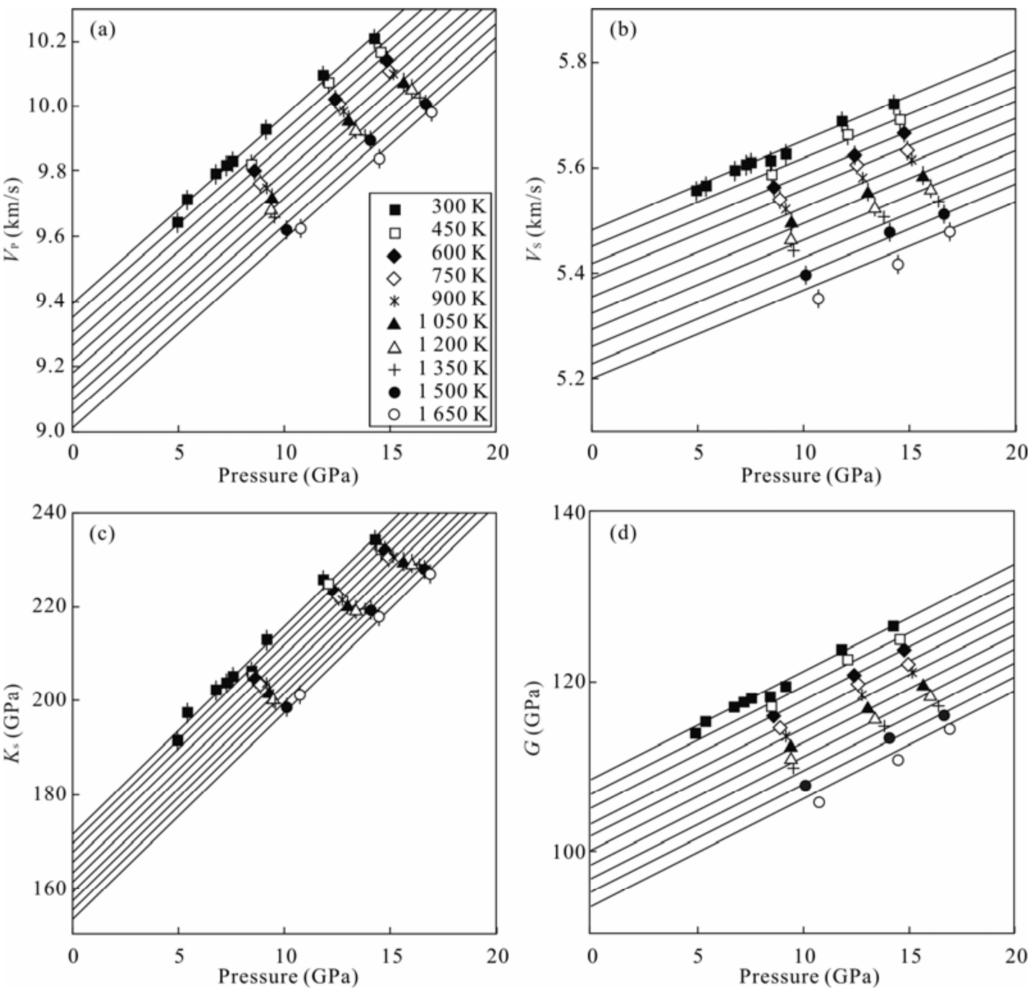

Figure 3. P-wave (V_P) and S-wave (V_S) velocities, and adiabatic bulk (K_S), and shear (G) modulus of grossular as functions of pressure and temperature. The lines are calculated from the two-dimensional linear fitting, and the parameters are described in the text. Vertical lines represent uncertainties.

Figure 4 shows pressure dependence of K_S and G at 300 K. Our predicted K_S and G at 0 GPa is similar to those measured at ambient pressure (K_{S0}=168.4(7) and G_0=108.9(4), Bass, 1989). Our obtained G value shows a linear increase with increasing pressure, although the G values of Conrad et al. (1999) are scattered. Similarly to G, K_S values linearly increase with increasing pressure. Our data show that $\partial K_S/\partial P$ value is apparently higher than 4 but is lower than 5 (Fig. 4a). Our obtained K_S value is similar to those of Conrad et al. (1999) up to 7 GPa, while Conrad et al. (1999) showed markedly higher K_S than this study at 7.7 and 10.0 GPa. To satisfy the high K_S value of Conrad et al. (1999), a $\partial K_S/\partial P$ value higher than 5 ($\partial K_S/\partial P$=5.46 by Conrad et al., 1999) is required. However, such a high $\partial K_S/\partial P$ value is inconsistent with our K_S value.

We compared the pressure-volume data obtained in several previous studies (Pavese et al., 2001; Zhang et al., 1999; Olijnyk et al., 1991; Weaver et al., 1976). We estimated isothermal bulk modulus (K_{T0}) and its pressure derivative (K_{T0}') from K_S and $\partial K_S/\partial P$ with the following equations

$$K_{T0}=K_{S0}/(1+\alpha\gamma T)$$

$$K_{T0}'=[(\partial K_S/\partial P)+q\alpha\gamma T-\gamma T(\partial K_T/\partial T)/K_{T0}]/(1+\alpha\gamma T)$$

where α, γ, and q are the thermal expansion coefficient, the Grüneisen parameter, and the volume dependence of the Grüneisen parameter, respectively. We used the $\partial K_S/\partial P$ value observed by the linear fitting for K_S data at several pressure and temperature conditions. We adopted the α, γ, q, and $\partial K_T/\partial T$ values of 3.12×10^{-5} K^{-1} (Pavese et al., 2000), 1.08, 0.4 (Stixrude and Lithgow-Bertelloni, 2005), and -0.02 GPa/K (Isaak et al., 1992), respectively. The equations

Table 1 Experimentally determined unit-cell volume (*V*), density (*ρ*), P- (V_P), and S-wave (V_S) velocities, adiabatic bulk (K_S) and shear (*G*) modulus of grossular at high pressures (*P*) up to 16.9 GPa and temperatures (*T*) between 300 and 1 650 K

T (K)	P (GPa)	V (Å^3)	ρ (g/cm^3)	V_P (km/s)	V_S (km/s)	K_S (GPa)	G (GPa)
300	4.93(2)	1 620.79(12)	3.692 1(3)	9.64(3)	5.55(1)	191.5(23)	113.9(6)
300	5.39(2)	1 608.72(12)	3.719 8(3)	9.72(3)	5.57(1)	197.4(24)	115.3(6)
300	6.76(3)	1 601.80(14)	3.735 9(3)	9.79(3)	5.60(1)	202.2(24)	117.0(6)
300	7.26(2)	1 599.03(12)	3.742 4(3)	9.82(3)	5.61(1)	203.9(24)	117.6(6)
300	7.54(3)	1 596.61(11)	3.748 0(3)	9.83(3)	5.61(1)	205.2(25)	117.9(6)
300	8.44(4)	1 594.94(16)	3.752 0(4)	9.85(3)	5.61(1)	206.4(25)	118.2(6)
300	9.17(2)	1 585.51(11)	3.774 3(3)	9.93(3)	5.63(1)	212.9(26)	119.4(6)
300	11.82(3)	1 562.29(9)	3.830 4(2)	10.10(3)	5.69(1)	225.6(27)	123.8(6)
300	14.27(4)	1 547.61(11)	3.866 7(3)	10.21(3)	5.72(1)	234.2(28)	126.5(7)
450	8.47(3)	1 595.87(12)	3.749 8(3)	9.82(3)	5.59(1)	205.7(25)	117.0(6)
450	12.09(2)	1 564.29(10)	3.825 5(3)	10.08(3)	5.66(1)	224.9(27)	122.6(6)
450	14.54(3)	1 550.20(15)	3.860 3(4)	10.17(3)	5.69(1)	232.5(28)	125.0(7)
600	8.60(4)	1 597.53(17)	3.745 9(4)	9.80(3)	5.56(1)	204.8(25)	116.0(6)
600	12.40(2)	1 567.12(10)	3.818 6(3)	10.02(3)	5.62(1)	222.7(27)	120.8(6)
600	14.78(3)	1 552.55(15)	3.854 4(4)	10.14(3)	5.67(1)	231.7(28)	123.7(6)
750	8.87(3)	1 600.85(17)	3.738 1(4)	9.76(3)	5.54(1)	203.5(24)	114.6(6)
750	12.56(1)	1 569.47(12)	3.812 8(3)	10.01(3)	5.61(1)	222.3(27)	119.8(6)
750	14.93(3)	1 555.17(15)	3.847 9(4)	10.11(3)	5.63(1)	230.5(28)	122.1(6)
900	9.15(2)	1 604.59(14)	3.729 4(3)	9.75(3)	5.52(1)	202.9(24)	113.6(6)
900	12.77(1)	1 572.68(12)	3.805 1(3)	9.98(3)	5.58(1)	221.2(27)	118.5(6)
900	15.13(2)	1 557.21(12)	3.842 9(3)	10.10(3)	5.61(1)	230.8(28)	121.2(6)
1 050	9.40(3)	1 607.79(12)	3.722 0(3)	9.72(3)	5.50(1)	201.7(24)	112.5(6)
1 050	13.01(1)	1 578.41(10)	3.791 3(2)	9.96(3)	5.55(1)	220.2(26)	116.9(6)
1 050	15.64(2)	1 560.07(16)	3.835 8(4)	10.08(3)	5.59(1)	229.8(28)	119.7(6)
1 200	9.39(4)	1 611.01(14)	3.714 5(3)	9.69(3)	5.47(1)	200.4(24)	111.0(6)
1 200	13.35(1)	1 578.40(10)	3.791 3(2)	9.93(3)	5.53(1)	219.4(26)	115.8(6)
1 200	16.00(2)	1 562.98(15)	3.828 7(4)	10.06(3)	5.56(1)	229.2(28)	118.4(6)
1 350	9.52(3)	1 613.99(15)	3.707 7(3)	9.66(3)	5.44(1)	199.5(24)	109.8(6)
1 350	13.79(1)	1 580.86(11)	3.785 4(3)	9.91(3)	5.51(1)	219.0(26)	114.7(6)
1 350	16.37(2)	1 565.28(17)	3.823 1(4)	10.03(3)	5.54(1)	228.2(27)	117.1(6)
1 500	10.09(1)	1 617.89(20)	3.698 7(5)	9.62(3)	5.40(1)	198.6(24)	107.8(6)
1 500	14.06(1)	1 583.70(10)	3.778 6(2)	9.90(3)	5.48(1)	219.2(26)	113.3(6)
1 500	16.64(2)	1 567.54(15)	3.817 6(4)	10.01(3)	5.51(1)	228.0(27)	116.0(6)
1 650	10.71(1)	1 620.02(22)	3.693 9(5)	9.62(3)	5.35(1)	201.2(24)	105.7(5)
1 650	14.46(2)	1 585.82(11)	3.773 5(2)	9.84(3)	5.42(1)	217.7(26)	110.7(6)
1 650	16.91(3)	1 570.10(16)	3.811 3(4)	9.98(3)	5.48(1)	227.2(27)	114.4(6)

The number in parentheses represents uncertainties in the last digit.

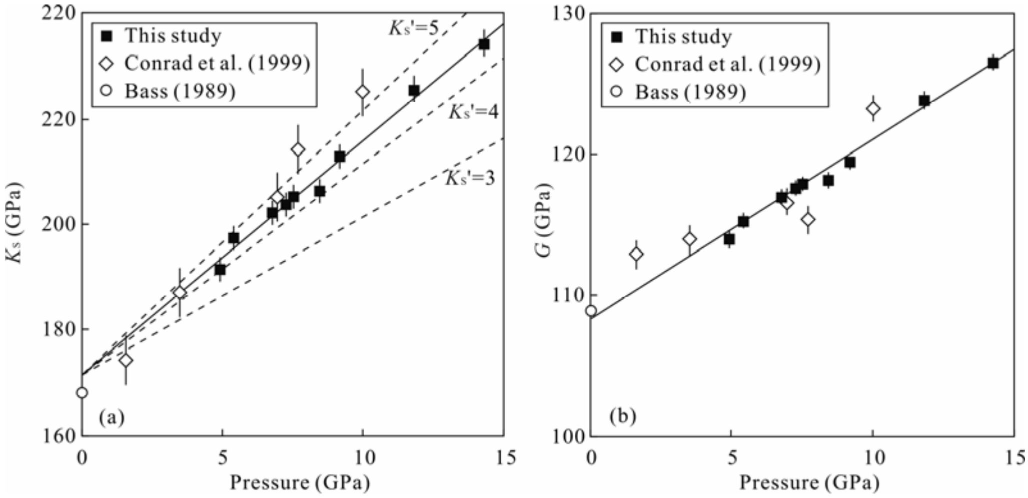

Figure 4. Pressure dependence of K_S (a) and G (b) at 300 K compared with those of a previous study (Conrad et al., 1999). K_S and G at room pressure and temperature condition (Bass, 1989) are plotted for reference. Vertical lines represent uncertainties.

yielded K_{T0} and K_{T0}' values of 170.0(8) GPa and 4.43(7), respectively, which are only slightly changed (less than 0.9 %) from the adiabatic value. The K_{T0} is similar to that of previous studies (e.g., K_{T0}=170(4), Zhang et al., 1999; K_{T0}=168.2(17), Pavese et al., 2001), although the K_{T0}' value differs from those of Zhang et al. (1999) and Pavese et al. (2001).

Then pressure was determined from the third-order Birch-Murnaghan equation-of-state (e.g., Birch, 1952)

$$P(V, 300\ \text{K})=3K_{T0}(1+2f)^{5/2}f[1+3(K_{T0}'-4)f/2]$$

where $f=[(V/V_0)^{-2/3}-1]/2$.

We adopted the V_0 value of 1 664.1 Å^3 obtained by single crystal X-ray diffraction at ambient pressure (Roderhorst et al., 2002). Estimated pressure-volume relation at 300 K is consistent with the volume data obtained in previous studies (Pavese et al., 2001; Zhang et al., 1999; Olijnyk et al., 1991; Weaver et al., 1976) (Fig. 5). Although the volume data of Weaver et al. (1976) and Olijnyk et al. (1991) slightly scatter, the data were plotted along the pressure-volume line estimated in this study. Because the pressure-volume data of grossular are consistent among this study and previous studies, the disagreements of the K_{T0}' value in previous studies are not due to the differences of experimental methods such as the difference of pressure medium and/or pressure scale. Although Pavese et al. (2001) showed a small K_{T0}' value of less than 4, these volume data can be explained with our K_{T0}' value of 4.43. The small K_{T0}' value by Pavese et al. (2001) would be due to the limitation of the pressure range (up to 4.3 GPa). In fact, Pavese et al. (2001) showed large uncertainties in the K_{T0}' value (±1.76). Furthermore, higher-pressure volume measurements also show large uncertainties in the K_{T0}' value (higher than ±0.6) (Zhang et al., 1999; Olijnyk et al., 1991) (Table 2). If we take account of the large uncertainties in previous studies, our obtained K_{T0}' value is in good agreement with that of previous studies. Since bulk modulus is the derivative of a pressure-volume rela-

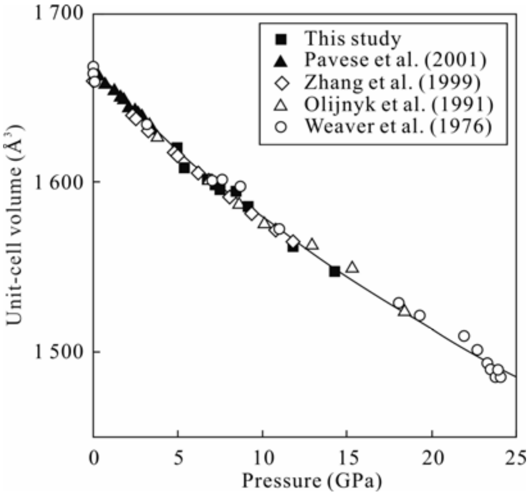

Figure 5. Pressure-volume relation of grossular at 300 K obtained in this study and previous studies (Pavese et al., 2001; Zhang et al., 2001; Olijnyk et al., 1991; Weaver et al., 1976). The line represents predicted pressure-volume relation from the bulk modulus derived by our V_P and V_S measurements.

tion and K_{T0}' is the further pressure derivative of bulk modulus, it would be difficult to constrain the K_{T0}' value of grossular from pressure-volume measurements. Difficulty in the determination of K_{T0}' value from pressure-volume measurement would be the cause of the disagreements of K_{T0}' values in previous studies.

Figure 6 shows a decrement of K_S and G as a function of temperature at 0 GPa. The temperature dependence of K_S is consistent between this study and Isaak et al. (1992), while Isaak et al. (1992) showed a stronger temperature dependence of G than that of this study. Our calculated G value is 2.5 GPa higher than that measured by Isaak et al. (1992) at 1 350 K. Our temperature dependence of G at temperatures lower than ~600 K is comparable to that of Isaak et al. (1992). In contrast, Isaak et al. (1992) showed a nonlinear temperature dependence of G at high temperatures under ambient pressure condition. Our obtained G values do not show a notable nonlinear temperature dependence, while G values at 1 650 K are slightly lower than those calculated from linear fitting (Fig. 3). The difference in G at 1 650 K becomes larger with decreasing pressure. This might be an indication of the initiation of a nonlinear temperature dependence of G. These data imply that the nonlinear temperature dependence of G might be influenced by the pressure condition, and pressure would reduce the nonlinear temperature dependence of G of grossular.

Table 2 shows pressure and temperature dependences of K_S and G of garnets with several chemical compositions. Similarly to the data of grossular, Conrad et al. (1999) showed a significantly higher $\partial K_S/\partial P$ value than 5 for andradite, while they showed low $\partial K_S/\partial P$ value of 3.22 for pyrope. Although the work of Conrad et al. (1999) is the only study for the $\partial K_S/\partial P$ of andradite, $\partial K_S/\partial P$ of pyrope has been investigated by other experimentalists: Two recent studies showed $\partial K_S/\partial P$ of 4.1(3) (Sinogeikin and Bass, 2000) and 4.3(3) (Gwanmesia et al., 2006), which are inconsistent with that of Conrad et al. (1999). They studied $\partial K_S/\partial P$ of pyrope by using different high-pressure techniques and different measurement methods (Sinogeikin and Bass, 2000: Brillouin scattering measurement in diamond anvil cell, Gwanmesia et al., 2006: ultrasonic measurement in multi-anvil apparatus), and, therefore, the identical $\partial K_S/\partial P$ value of 4.1–4.3 for pyrope would be reliable. Limitation of

Table 2 Pressure and temperature dependences of bulk (K_S) and shear (G) modulus of garnets

Composition	K_{S0} (GPa)	G_0 (GPa)	$\partial K_S/\partial P$	$\partial G/\partial P$	$\partial K_S/\partial T$ (10^{-2} GPa/K)	$\partial G/\partial T$ (10^{-2} GPa/K)	References
Grossular	171.5(8)	108.4(3)	4.42(7)	1.27(3)	-1.36(5)	-1.11(2)	This study
	166.82	108.9	5.46	1.1			Ref. 1
	167.8(0.7)	107.0(0.2)			-1.49(1)	-1.25(1)**	Ref. 2
	168.6(20)*		3.42(176)*		-1.6(3)*		Ref. 3
	170(4)*		5.2(6)*				Ref. 4
	167.8(25)*		6.2(40)*				Ref. 5
Pyrope	171.2(20)	93.7(20)	4.1(3)	1.3(2)			Ref. 6
	172(2)	91(1)	4.3(3)	1.5(2)	-2.6(4)	-1.0(1)	Ref. 7
	171(2)	94(2)			-1.45(20)	-0.92(10)	Ref. 8
	172.73	92	3.22	1.4			Ref. 1
Andradite	159.38	90	5.85	4.3			Ref. 1
Pyrolitic garnet	164.4(5)	94.9(2)	4.24(6)	1.11(3)	-1.29(8)	-1.03(4)	Ref. 9
MORB garnet	155.8	93.2	4.5	1.5			Ref. 10

*. Isothermal value; **. 2nd order fit with a $\partial^2G/\partial T^2$=-2.1(1)×10^{-6} GPa/K. References: 1. Conrad et al., 1999; 2. Isaak et al., 1992; 3. Pavese et al., 2001; 4. Zhang et al., 1999; 5. Olijnyk et al., 1991; 6. Sinogeikin and Bass, 2000; 7. Gwanmesia et al., 2006; 8. Sinogeikin and Bass, 2002; 9. Irifune et al., 2008; 10. Kono et al., 2007. The number in parentheses represents uncertainty.

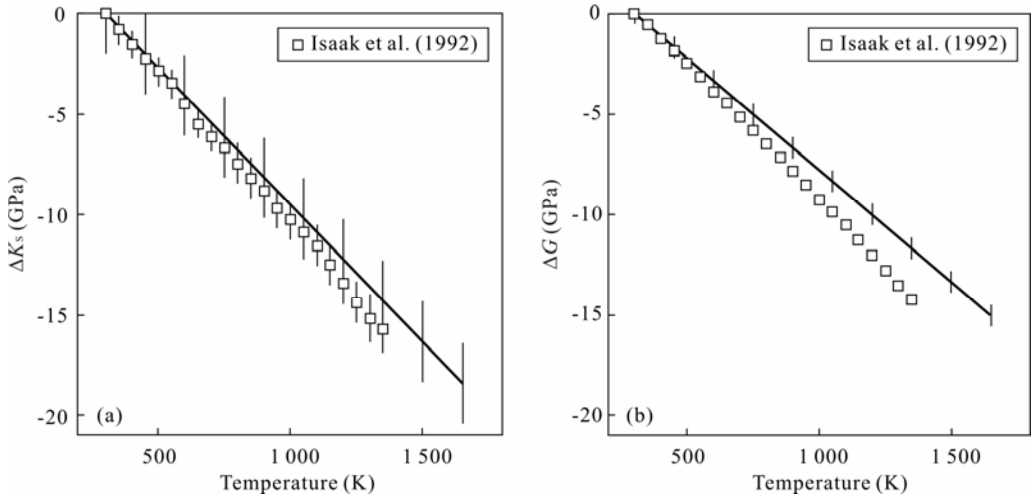

Figure 6. Decrement of K_S (ΔK_S) and G (ΔG) with increasing temperature at 0 GPa obtained directly by resonant ultrasonic spectroscopy at ambient pressure (Isaak et al., 1992) (open square) and predicted from our high-pressure and high-temperature measurements (solid line). Vertical lines represent uncertainties.

the data might yield such disagreements, as Conrad et al. (1999) investigated the elastic properties of the garnets only at 4–6 pressure conditions with a maximum pressure of 10 GPa.

Recent elastic property measurements show $\partial K_S/\partial P$ values of garnets of 4.0–4.5 (Table 2). Our determined $\partial K_S/\partial P$ value of grossular of 4.42(7) is similar to that of other garnets. $\partial G/\partial P$ value is similar among grossular, pyrope, and MORB garnets (1.3–1.5) except for garnet with a pyrolite minus olivine composition, which showed a smaller $\partial G/\partial P$ value of 1.1 (Irifune et al., 2008). Temperature dependences of the K_s ($\partial K_S/\partial T$) of garnets are ~(-1.3–1.5)×10^{-2} GPa/K except for the high $\partial K_S/\partial T$ of pyrope (-2.6×10^{-2} GPa/K) by Gwanmesia et al. (2006), and no marked compositional dependence was found. In contrast, the temperature dependence of G ($\partial G/\partial P$) of grossular is higher than those of pyrope and pyrolitic garnet ((-0.9)–(-1.0))×10^{-2} GPa/K). Although our $\partial G/\partial T$ value (-1.1×10^{-2} GPa/K) is markedly lower than that of Isaak et al. (1992), this value is still higher than those of pyrope and pyrolitic garnets. It has been reported that Mg end-member garnets ($Mg_3Al_2Si_3O_{12}$ pyrope and $MgSiO_3$ majorite) showed similar temperature dependence of K_S and G (Sinogeikin and Bass, 2002), and that the aluminum content does not influence the temperature dependence of K_S and G. In contrast, the data of this study and Isaak et al. (1992) suggest that the $\partial G/\partial T$ value depends on the calcium content, although $\partial K_S/\partial T$ value is not significantly influenced by the calcium content. The data imply that Ca-rich garnet such as garnet in MORB composition should have stronger temperature dependence of V_S than that of peridotite composition.

In addition, the nonlinear temperature dependence for G is one of the most ambiguous issues in understanding the temperature dependence of garnets. Isaak et al. (1992) and our data showed that the nonlinear temperature dependence of G of grossular is significant at ambient pressure, but reduced at high pressures of ~8–17 GPa. In contrast, Irifune et al. (2008) showed a notable nonlinear temperature dependence of G for pyrolitic garnet above ~1 000 K at high pressures of ~15–18 GPa. The data suggest that the initiation of the nonlinear decrease in G would also depend on composition. In order to clarify the nonlinear temperature dependence of G, we need further investigations on the temperature dependence of G of several different garnets at high pressures and high temperatures.

ACKNOWLEDGMENTS

We thank two anonymous reviewers and the editor for constructive comments and suggestions that improved this manuscript. This study was conducted based on a research proposal to SPring-8 by Y Kono (No. 2007B1648), supported by Grant-in-aid for Scientific Research from the Japanese government to T Irifune.

REFERENCES CITED

Bass, J. D., 1989. Elasticity of Grossular and Spessartite Garnets by Brillouin Spectroscopy. *J. Geophys. Res.*, 94(B6): 7621–7628

Birch, A. F., 1952. Elasticity and Constitution of the Earth's Interior. *J. Geophys. Res.*, 57(2): 227–286

Conrad, P. G., Zha, C. S., Mao, H. K., et al., 1999. The High-Pressure Single-Crystal Elasticity of Pyrope, Grossular, and Andradite. *Am. Min.*, 84: 374–383

Gwanmesia, G. D., Zhang, J. Z., Darling, K., et al., 2006. Elasticity of Polycrystalline Pyrope ($Mg_3Al_2Si_3O_{12}$) to 9 GPa and 1 000 ℃. *Phys. Earth Planet. Inter.*, 155(3–4): 179–190

Higo, Y., Inoue, T., Li, B. S., et al., 2006. The Effect of Iron on the Elastic Properties of Ringwoodite at High Pressure. *Phys. Earth Planet. Inter.*, 159(3–4): 276–285

Higo, Y., Kono, Y., Inoue, T., et al., 2009. A System for Measuring Elastic Wave Velocity under High Pressure and High Temperature Using a Combination of Ultrasonic Measurement and the Multi-anvil Apparatus at SPring-8. *J. Synchrotron Rad.*, 16: 762–768

Irifune, T., Higo, Y., Inoue, T., et al., 2008. Sound Velocities of Majorite Garnet and the Composition of the Mantle Transition Region. *Nature*, 451(7180): 814–817

Isaak, D., Anderson, O. L., Oda, H., 1992. High-Temperature Thermal Expansion and Elasticity of Calcium-Rich Garnets. *Phys. Chem. Minerals*, 19(2): 106–120

Kono, Y., Higo, Y., Ohfuji, H., et al., 2007. Elastic Wave Velocities of Garnetite with a MORB Composition up to 14 GPa. *Geophys. Res. Lett.*, 34(14): L14308, doi: 10.1029/2007GL030312

Li, B. S., Hung, J., Liebermann, R. C., 2004. Modern Techniques in Measuring Elasticity of Earth Materials at High Pressure and High Temperature Using Ultrasonic Interferometry in Conjunction with Synchrotron X-Radiation in Multi-anvil Apparatus. *Phys. Earth Planet. Inter.*, 143–144: 559–574

Nobes, R. H., Akhmatskaya, E. V., Milman, V., et al., 2000. Structure and Properties of Aluminosilicate Garnets and Katotite: An Ab Initio Study. *Computational Materials Science*, 17(2–4): 141–145

O'Neill, B., Bass, J. D., Rossman, G. R., et al., 1991. Elastic Properties of Pyrope. *Phys. Chem. Minerals*, 17(7): 617–621

O'Neill, B., Bass, J. D., Smyth, J. R., et al., 1989. Elasticity of a Grossular-Pyrope-Almandine Garnet. *J. Geophys. Res.*, 94(B12): 17819–17824

Olijnyk, H., Paris, E., Geiger, C. A., et al., 1991. Compressional Study of Katoite [$Ca_3Al_2(O_4H_4)_3$] and Grossular Garnet. *J. Geophys. Res.*, 96(B9): 14313–14318

Pavese, A., Diella, V., Pischedda, V., et al., 2001. Pressure-Volume-Temperature Equation of State of Andradite and Grossular, by High-Pressure and -Temperature Powder Diffraction. *Phys. Chem. Minerals*, 28(4): 242–248

Rodehorst, U., Geiger, C. A., Armbruster, T., et al., 2002. The Crystal Structures of Grossular and Spessartine between 100 and 600 K and the Crystal Chemistry of Grossular-Spessartine Solid Solutions. *Am. Min.*, 87: 542–549

Sinelnikov, Y. D., Chen, G. L., Liebermann, R. C., 2004. Dual Mode Ultrasonic Interferometry in Multi-anvil High Pressure Apparatus Using Single-Crystal Olivine as the Pressure Standard. *High Press. Res.*, 24(1): 183–191

Sinogeikin, S. V., Bass, J. D., 2000. Single-Crystal Elasticity of Pyrope and MgO to 20 GPa by Brillouin Scattering in the Diamond Cell. *Phys. Earth Planet. Inter.*, 120(1–2): 43–62

Sinogeikin, S. V., Bass, J. D., 2002. Elasticity of Majorite and a Majorite-Pyrope Solid Solution to High Pressure: Implications for the Transition Zone. *Geophys. Res. Lett.*, 29(2): 1017, doi:10.1029/2001GL013937

Stixrude, L., Lithgow-Bertelloni, C., 2005. Thermodynamics of Mantle Minerals—I, Physical Properties. *Geophys. J. Int.*, 162(2): 610–632

Tsuchiya, T., 2003. First-Principles Prediction of the *P-V-T* Equation of State of Gold and the 660-km Discontinuity in Earth's Mantle. *J. Geophys. Res.*, 108(B10): 2462, doi:10.1029/2003JB002446

Wang, Y. B., Weidner, D. J., Zhang, J. Z., et al., 1998. Thermal Equation of State of Garnets along the Pyrope-Majorite Join. *Phys. Earth Planet. Inter.*, 105(1–2): 59–72

Weaver, J. S., Takahashi, T., Bass, J. D., 1976. Isothermal Compression of Grossular Garnets to 250 kbar and the Effect of Calcium on the Bulk Modulus. *J. Geophys. Res.*, 81(14): 2475–2482

Zhang, L., Ashbahs, H., Kutoglu, A., et al., 1999. Single-Crystal Hydrostatic Compression of Synthetic Pyrope, Almandine, Spessartine, Grossular and Andradite Garnets at High Pressures. *Phys. Chem. Minerals*, 27(1): 52–58